Mech Time-Depend Mater (2013) 17:465–479
DOI 10.1007/s11043-012-9197-6

Relaxation modulus—complex modulus interconversion for linear viscoelastic materials

Jon García-Barruetabeña · Fernando Cortés · José Manuel Abete · Pelayo Fernández · María Jesús Lamela · Alfonso Fernández-Canteli

Received: 23 January 2012 / Accepted: 5 October 2012 / Published online: 25 October 2012

Abstract This paper is aimed at exploring the interconversion path between the relaxation modulus $E(t)$ and the corresponding complex modulus $E^*(\omega)$ for linear viscoelastic solid materials. In contrast to other approximate methods, the fast Fourier transform (FFT) algorithm is directly applied on the time-dependent part of the viscoelastic response $R(t)$. Firstly, the method foundations are presented. Then, a theoretical example is performed by means of a generalized Maxwell model, where the influence of sampling conditions and eventual experimental error and data dispersion is analyzed. Finally, an application example using experimental data is carried out to assess the method. As a result, the proposed procedure allows obtaining the complex modulus by means of relaxation tests, and vice versa.

J. García-Barruetabeña (✉)
Department of Mechanical Engineering, Ikerlan-IK4, J.M. Arizmendiarrieta 2, 20500 Mondragón, Spain
e-mail: jgarcia@ikerlan.es

F. Cortés
Deusto Institute of Technology (DeustoTech), Faculty of Engineering, University of Deusto, Avenida de las Universidades 24, 48007 Bilbao, Spain
e-mail: fernando.cortes@deusto.es

J.M. Abete
Department of Mechanical Engineering, Mondragon Unibertsitatea, Loramendi 4, 20500 Mondragón, Spain
e-mail: jmabete@mondragon.edu

P. Fernández · M.J. Lamela · A. Fernández-Canteli
Department of Construction and Manufacturing Engineering, University of Oviedo, Campus de Viesques, 33203 Gijón, Spain

P. Fernández
e-mail: fenandezpelayo.uo@uniovi.es

M.J. Lamela
e-mail: mjesuslr@uniovi.es

A. Fernández-Canteli
e-mail: afc@uniovi.es

Keywords Relaxation modulus · Complex modulus · Viscoelasticity · Material functions interconversion

1 Introduction

Viscoelastic materials (VEM) are widely employed in engineering applications and their spread is growing in many sectors such as automotive industry, aerospace, wind power, human transportation, etc. VEM mechanical properties depend on temperature, frequency and amplitude, pre-stress, dynamic load level, relative humidity, among others (Ward and Sweeney 2004). Service temperature, frequency and amplitude of deformation are the most relevant ones (Sjöberg and Kari 2003). Thus, proper mechanical characterization is essential in order to obtain reliable predictions (Warnaka and Miller 1968).

Concerning VEM behavior modeling, the memory of viscoelastic materials can be properly represented using the Boltzmann superposition principle (Boltzmann 1876). Therefore, time evolution of stress $\sigma(t)$ can be evaluated using relaxation functions $R(t)$ through convolution integrals given by

$$\sigma(t) = E_{\mathrm{r}}\varepsilon(t) + \int_0^t R(t-\lambda)\dot{\varepsilon}(\lambda)\,\mathrm{d}\lambda, \tag{1}$$

where $\varepsilon(t)$ is strain, E_{r} the viscoelastic constant, λ the integration variable and $(\dot{\bullet})$ represents time derivative. In frequency domain, viscoelastic behavior can be represented by the complex modulus approximation (Nashif et al. 1985),

$$E^*(\omega) = E'(\omega) + \mathrm{i}E''(\omega) = E'(\omega)\big[1 + \mathrm{i} \times \tan\delta(\omega)\big], \tag{2}$$

where $E'(\omega)$ is the storage modulus, $E''(\omega)$ the loss modulus, $\mathrm{i} = \sqrt{-1}$, and $\tan\delta(\omega)$ is the loss factor, which is defined as

$$\tan\delta(\omega) = \frac{E''(\omega)}{E'(\omega)}. \tag{3}$$

Concerning VEM experimental characterization, ASTM E 756-04 (ASTM 2004) details the methodology to characterize the mechanical behavior of non-self-supporting viscoelastic materials, implying the use of multimaterial Oberst beam specimens. Nevertheless, the main inconvenience of this standard consists in introducing additional damping or mass through excitation or measurement devices. Besides, it should be remarked that standard methods give glass transition temperature T_{g} values, which are not accurate for given moduli and the true measure of damping.

In this context, DMTA technique allows to take into account together temperature and time (or temperature and frequency) by means of the time-temperature superposition (TTS) principle (Ferry 1980) introducing no extra mass or damping.

Thus, frequency-time interconversion methods are valuable and useful tools (Emri and von Bernstorff 2005; Park and Schapery 1999a, 1999b) due to the fact that they can also be applied to overcome the inherent difficulties of relaxation or dynamic characterizations (Kulik et al. 2009; Maheri and Adams 2002; Jahani and Nobari 2008), depending on the tested material. The most widely applied methods (Emri and von Bernstorff 2005) for material functions conversion from time to frequency domains are those based on Prony series (Chen 2000), and the opposed conversion can be achieved through the algorithms proposed by Ninomiya and Ferry (1959). The former can be obtained by fitting the experimental data by means of a generalized Maxwell model (Fernández et al. 2011), whereas the latter

is based on experimental data fitting. Both conversion methods are approximate. Nevertheless, the methods proposed by Schwarzl (1970) should be highlighted also since both interconversions can be achieved. More recently, other authors have proposed other methods (Emri and von Bernstorff 2005; Park and Schapery 1999a, 1999b; Kulik et al. 2009; Maheri and Adams 2002; Jahani and Nobari 2008; Chen 2000; Ninomiya and Ferry 1959; Fernández et al. 2011; Schwarzl 1970; Sorvari and Malinen 2007). Nevertheless, that of Leblanc (2005) should be highlighted, as his work focuses on the employment of the Fourier transform but in order to investigate non-linear viscoelastic materials. As the author states (Leblanc 2005), standard dynamic testing requires strict proportionality between strain and stress for valid resolution of the experimental complex modulus into its elastic and viscous components. Nevertheless, no such condition is needed when the Fourier transform is employed.

In short, the main objective of the present paper is to explore a unique interconversion method between time and frequency domains in order to obtain the complex modulus $E^*(\omega)$ by means of relaxation tests, and vice versa. The advantage of this method is a direct employment of the fast Fourier transform (FFT) algorithm to experimental data, in opposition to other existing methods (Emri and von Bernstorff 2005; Park and Schapery 1999a, 1999b; Kulik et al. 2009; Maheri and Adams 2002; Jahani and Nobari 2008; Chen 2000; Ninomiya and Ferry 1959; Fernández et al. 2011; Schwarzl 1970; Sorvari and Malinen 2007) based on fitting models or theoretical functions. Concretely, the proposed method is valuable when a Prony series cannot be properly fitted to the experimental data in time or frequency domains. This article is structured as follows:

- Firstly, the method foundations are presented.
- Then, a theoretical example is performed by means of a generalized Maxwell model, where the influence of the sampling conditions and the eventual experimental error data dispersion is analyzed.
- Finally, an application example using experimental data is carried out to assess the method.

2 Method foundations

An experimental relaxation test consists of applying a strain step as $\varepsilon(t) = \varepsilon_0 \mathrm{H}(t)$, where ε_0 is the magnitude of the strain and $\mathrm{H}(t)$ is the Heaviside function. Consequently, applying a strain step and substituting its time derivative to (1), yields

$$\sigma(t) = E_\mathrm{r}\varepsilon_0 \mathrm{H}(t) + \int_0^t R(t-\lambda)\varepsilon_0 \delta(\lambda)\,\mathrm{d}\lambda = \big[E_\mathrm{r} + R(t)\big]\varepsilon_0, \tag{4}$$

where $\delta(t)$ is the Dirac function. Then, the relaxation modulus $E(t)$ can be deduced as

$$E(t) = \frac{\sigma(t)}{\varepsilon_0} = E_\mathrm{r} + R(t), \tag{5}$$

where the viscoelastic constant E_r is the long-term part of the relaxation modulus and $R(t)$ is the time-dependent one.

Next, by means of the Fourier transform, the complex modulus $E^*(\omega)$ is obtained. On the one hand, applying the Fourier transform to Eq. (5) results in

$$\tilde{E}(\omega) = \frac{E_\mathrm{r}}{\mathrm{i}\omega} + \tilde{R}(\omega), \tag{6}$$

where $(\tilde{\bullet})$ represents the Fourier transform. On the other hand, applying the Fourier transform to Eq. (1) yields

$$\tilde{\sigma}(\omega) = E_{\mathrm{r}}\tilde{\varepsilon}(\omega) + \mathrm{i}\omega\tilde{R}(\omega)\tilde{\varepsilon}(\omega), \tag{7}$$

from where the complex modulus $E^*(\omega)$ can be derived, yielding

$$E^*(\omega) = E_{\mathrm{r}} + \mathrm{i}\omega\tilde{R}(\omega). \tag{8}$$

Therefore, by substituting the Fourier transform of the time-dependent part of the viscoelastic response $\tilde{R}(\omega)$ to Eq. (6), a relationship between complex modulus $E^*(\omega)$ and the Fourier transform of the relaxation modulus $\tilde{E}(\omega)$ is obtained:

$$E^*(\omega) = \mathrm{i}\omega\tilde{E}(\omega). \tag{9}$$

It can be concluded that the complex modulus $E^*(\omega)$ of a linear viscoelastic material can be computed from the Fourier transform of its relaxation modulus $E(t)$. However, employing the fast Fourier transform (FFT) algorithm, the resulting complex modulus $E^*(\omega)$ will suffer from leakage since $E(t)$ is not periodic (Bellanger 1984) and $E(t) \underset{t\to\infty}{=} E_{\mathrm{r}} \neq 0$. Consequently, to avoid leakage, it has to be taken into account that the viscoelastic component represented by the time-dependent part of the viscoelastic response $R(t)$ disappears with time, $R(t) \underset{t\to\infty}{=} 0$, thus FFT algorithm does not produce leakage on approximation of complex modulus $E^*(\omega)$ if Eq. (8) is used instead of (9). The disadvantage of the method is that the viscoelastic constant E_{r} is being obtained from the experimental data.

3 Theoretical example

In this section the influence of sampling conditions and eventual experimental error and data dispersion are analyzed by means of an exponential material model. The analysis is focused on several aspects related to the FFT algorithm: leakage, signal discretization and the analyzed ranges. In this work, the FFT algorithm proposed by Cooley and Tuckey (1965) to compute the discrete Fourier transform is employed (Oran 1988). This algorithm has some widely known disadvantages. These are: 2^n data points are needed; these points need to be evenly spaced (Oran 1988). Nevertheless, because of the wide range of applications based on the Fourier transform, many authors have developed several methods to overcome these requirements. Dutt and Rokhlin (1995) proposed a group of algorithms generalizing the FFT algorithm to the case of unevenly spaced data that have been applied to a wide range of applications (Fourmont 2003; Greengard and Lee 2004; Marion 2005; Lee and Greengard 2005). Nevertheless, as previously mentioned, the algorithm proposed by Cooley and Tuckey (1965) will be employed, because the other mentioned algorithms make use of resampling at different stages of the computation. Besides, it should be pointed out that regarding the FFT algorithm requirements, a single zero has been added to the experimental data in order to provide information for $t = 0$.

Exponential damping model is widely used in literature (Adhikari 2000, 2001) because of its capability to model damping mechanisms arising from viscoelastic nature of materials. Its time-dependent part of the viscoelastic response $R(t)$ is given by

$$R(t) = c\mu\mathrm{e}^{-\mu t}, \tag{10}$$

resulting in a relaxation modulus

$$E(t) = E_{\mathrm{r}} + E_1\mathrm{e}^{-\mu t}, \tag{11}$$

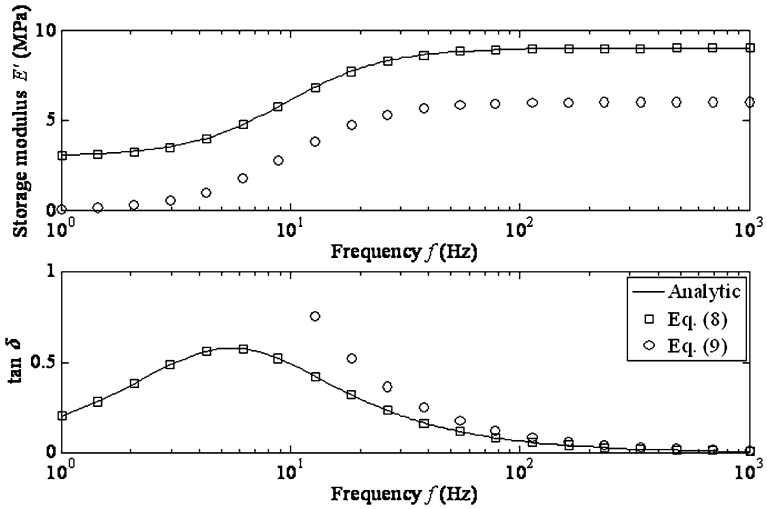

Fig. 1 Influence of leakage, conversion from time to frequency. Comparison among the analytic generalized Maxwell model complex modulus $E^*(\omega)$ provided by Eq. (13), the one computed by means of Eq. (9) and therefore suffering leakage, and the one computed by means of Eq. (8) and therefore avoiding leakage

where $\mu = \tau_{\mathrm{m}}^{-1} = E_1/c$ is the material relaxation parameter, τ_{m} the relaxation time, and E_1 and c are respectively stiffness and damping coefficient. The Fourier transform $\tilde{R}(\omega)$ of the time-dependent part of the viscoelastic response $R(t)$ is given by

$$\tilde{R}(\omega) = E_1 \frac{1}{\mu + \mathrm{i}\omega}. \tag{12}$$

Accordingly, the complex modulus $E^*(\omega)$ yields

$$E^*(\omega) = E_{\mathrm{r}} + E_1 \frac{\mathrm{i}\omega}{\mu + \mathrm{i}\omega}, \tag{13}$$

from where the storage modulus E' and the loss factor $\tan\delta$ can be directly obtained:

$$E'(\omega) = E_{\mathrm{r}} + E_1 \frac{\omega^2}{\mu^2 + \omega^2} \tag{14}$$

and

$$\tan\delta(\omega) = \frac{E_1 \mu \omega}{E_{\mathrm{r}}\mu^2 + E_1(\mu^2 + \omega^2)}. \tag{15}$$

For the numerical application, it is considered that $E_{\mathrm{r}} = 3$ MPa, $E_1 = 6$ MPa, and $c = 0.1$ MPa s.

3.1 Leakage

Next, the leakage influence is analyzed. For the conversion from time to frequency, the methods exposed in Sect. 2 are employed, comparing the exact complex modulus (13) with those provided by Eqs. (9) and (8). All the complex moduli are represented in Fig. 1 as storage modulus E' and loss factor $\tan\delta$.

From Fig. 1 it should be remarked that the direct use of Eq. (9) derives in erroneous results due to leakage, while through Eq. (8) the complex modulus $E^*(\omega)$ can be precisely computed from the relaxation modulus.

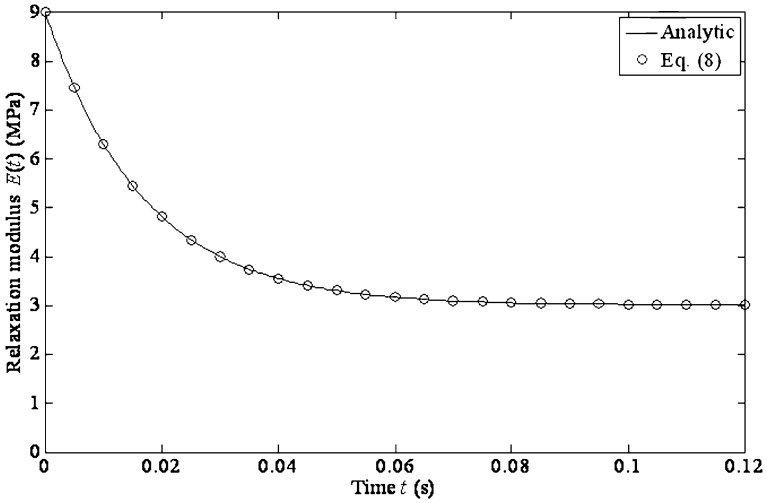

Fig. 2 Influence of leakage, conversion from frequency to time. Comparison between the analytic generalized Maxwell model relaxation modulus $E(t)$ provided by Eq. (11) and the one computed through Eq. (8) avoiding leakage

Considering the inverse transformation, the exact relaxation modulus given by Eq. (11) is compared with those provided by the inverse FFT applied on Eqs. (9) and (8). Unfortunately, the leakage resulting from (9) provides a numerical unstability, the relaxation modulus being infinity for every time. Therefore, Fig. 2 illustrates only two curves instead of three: the analytic response given by Eq. (11) and the estimation for $E(t)$ by means of Eq. (8).

From Fig. 2 it should be pointed out that the proposed procedure is capable of accurately computing the relaxation modulus $E(t)$, if the corresponding complex modulus $E^*(\omega)$ is known.

3.2 Influence of time and frequency sampling

Next, the influence of the time and frequency sampling is studied. It should be remembered that concerning the conversion from time to frequency of a function defined up to a maximum time $t_{\max}$, the discretization time Δt determines the Nyquist frequency $f_{\max}$ according to

$$f_{\max} = \frac{1}{2\Delta t}, \tag{16}$$

the resulting discretized frequency being

$$\Delta f = \frac{1}{t_{\max}}, \tag{17}$$

having

$$N = \frac{t_{\max}}{\Delta t} \tag{18}$$

discrete data.

Considering the inverse transformation from frequency to time, these three equations can be inversely taken into account.

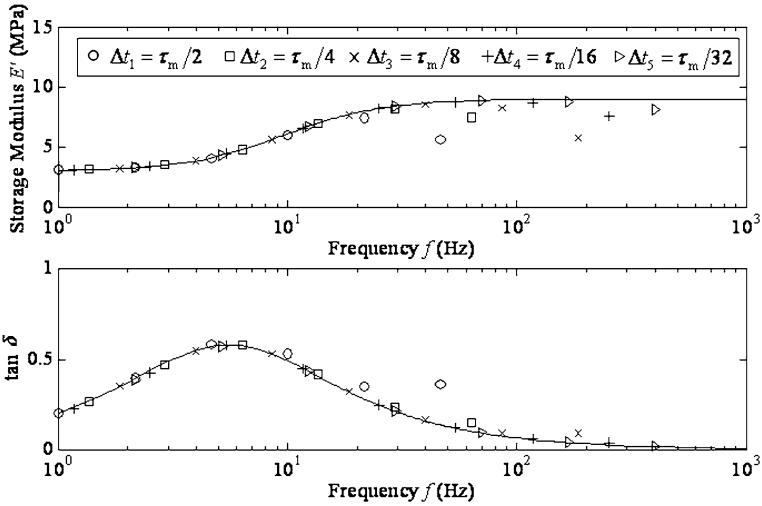

Fig. 3 Influence of sampling frequency, conversion from time to frequency. Comparison between generalized Maxwell model complex modulus $E^*(\omega)$ provided by Eq. (13) and the result provided by the proposed interconversion method for different sampling times

For the present analysis, $t_{\max} = 0.5$ s is chosen, and five different discretizations are considered: $\Delta t_1 = \tau_m/2 = 0.0083$ s, $\Delta t_2 = \tau_m/4 = 0.0042$ s, $\Delta t_3 = \tau_m/8 = 0.0021$ s, $\Delta t_4 = \tau_m/16 = 0.0010$ s and $\Delta t_5 = \tau_m/32 = 0.0005$ s. Therefore, Fig. 3 shows six curves: the five analyzed cases, plus the analytic response given by Eq. (13).

From Fig. 3 it should be noted that the lower is Δt, the higher is $f_{\max}$ and the better is the accuracy. Thus, $\Delta t_1 = \tau_m/2$ is only able to represent the low-frequency range, i.e. the rubbery zone and the beginning of the transition zone of the viscoelastic material (Ferry 1980). On the contrary, $\Delta t_5 = \tau_m/32$ is sufficient to accurately represent the complex modulus $E^*(\omega)$ in the whole frequency range, including the vitreous one (Ferry 1980).

Considering the inverse transformation, from frequency to time domain, a maximum frequency $f_{\max} = 1$ kHz is taken into account, and four discretization cases are analyzed: $\Delta f_1 = \tau_m^{-1}/2 = 29.94$ Hz, $\Delta f_2 = \tau_m^{-1}/4 = 14.97$ Hz, $\Delta f_3 = \tau_m^{-1}/8$ Hz $= 7.48$ Hz, and $\Delta f_4 = \tau_m^{-1}/16$ Hz $= 3.74$ Hz. Therefore, Fig. 4 shows five curves: the four analyzed cases and the analytic response given by (11).

From Fig. 4 it should be noted that in two of the considered cases, $\Delta f_1 = \tau_m^{-1}/2$ and $\Delta f_2 = \tau_m^{-1}/4$, the relaxation is not properly represented. Thus, differences are verified for $t < 0.02$ s. Consequently, they are not useful to compute the relaxation modulus $E(t)$. Considering the cases $\Delta f_3 = \tau_m^{-1}/8$ and $\Delta f_4 = \tau_m^{-1}/16$, the relaxation is reached, providing similar accuracy. Consequently, for the present case, a $\Delta f_3 = \tau_m^{-1}/8$ is small enough to accurately compute the relaxation modulus $E(t)$.

3.3 Influence of the maximum time and frequency

In this section, the influence of $t_{\max}$ and $f_{\max}$ is studied. First, the conversion from time to frequency is analyzed. The previously defined function discretization parameter Δt_5 is employed. Five truncated signals are considered: $t_{\max,1} = 2\tau_m = 0.0334$ s, $t_{\max,2} = 4\tau_m = 0.0668$ s, $t_{\max,3} = 8\tau_m = 0.1336$ s, $t_{\max,4} = 16\tau_m = 0.2672$ s and $t_{\max,5} = 32\tau_m = 0.5344$ s.

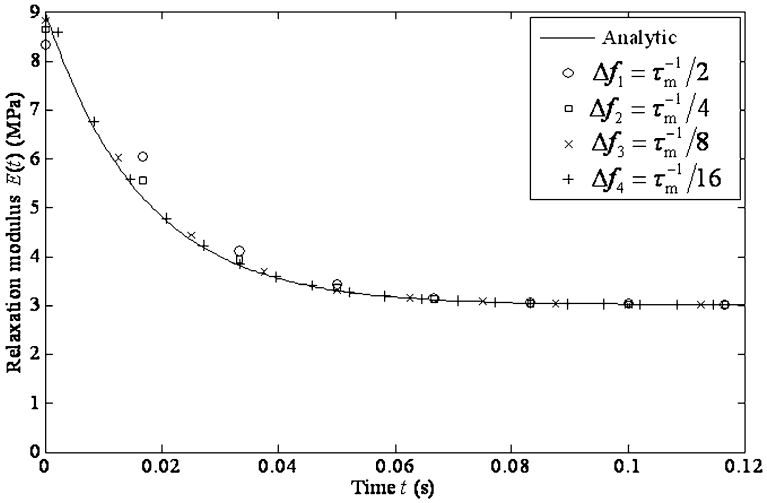

Fig. 4 Influence of sampling frequency, conversion from frequency to time. Comparison between generalized Maxwell model relaxation modulus $E(t)$ provided by Eq. (11) and the result provided by the proposed interconversion method for different sampling frequencies

On the one hand, Fig. 5(a) illustrates the exact $E(t)$ given by Eq. (11), in which each employed truncation is represented. On the other hand, Fig. 5(b) contains six curves corresponding to the five analyzed cases, plus the analytic response given by Eq. (13).

From Fig. 5(a) it should be remarked that in two of the considered cases, $t_{\max,1}$ and $t_{\max,2}$, the relaxation has not been reached, implying that only the vitreous zone can be represented, as Fig. 5(b) shows. Even if for $t_{\max,3}$ and $t_{\max,4}$ the relaxation has been reached, only the transition zone can be represented. In fact, to include the rubbery zone, a maximum spam $t_{\max,5}$ has to be taken into account.

Next, for the conversion from the complex modulus to the relaxation modulus, a previously defined discretization frequency Δf_3 is chosen. Three cases of maximum frequency are analyzed: $f_{\max,1} = 0.1\tau_m^{-1} \approx 6$ Hz, $f_{\max,2} = \tau_m^{-1} \approx 60$ Hz and $f_{\max,3} = 10\tau_m^{-1} \approx 600$ Hz, covering the rubbery, transition and vitreous zones, respectively, as Fig. 6(a) illustrates. Therefore, Fig. 6(b) represents four curves corresponding to the three analyzed cases, plus the analytic response given by Eq. (11).

From Fig. 6(b) it should be remarked that the higher is $f_{\max}$, the better is the accuracy. Consequently, $f_{\max,1} = 0.1\tau_m^{-1} \approx 6$ Hz is not able to represent the relaxation modulus $E(t)$. Concerning $f_{\max,2} = \tau_m^{-1} \approx 60$ Hz, differences are encountered during the relaxation until the viscoelastic constant E_r is reached. On the contrary, $f_{\max,3} = 10\tau_m^{-1} \approx 600$ Hz is sufficient to accurately represent $E(t)$ in the whole time range.

3.4 Influence of experimental error and data

In this section, the accuracy of the interconversion is analyzed taking into account eventual data dispersion. In this context, some pseudo-experimental data for $\bar{E}(t)$ and $\bar{E}^*(\omega)$ have been generated evaluating Eqs. (11) and (13), respectively, in some unevenly spaced data points, in which random eventual errors $\alpha(t)$ and $\alpha^*(\omega)$ have been included:

$$\bar{E}(t) = E(t) + \alpha(t) \tag{19}$$

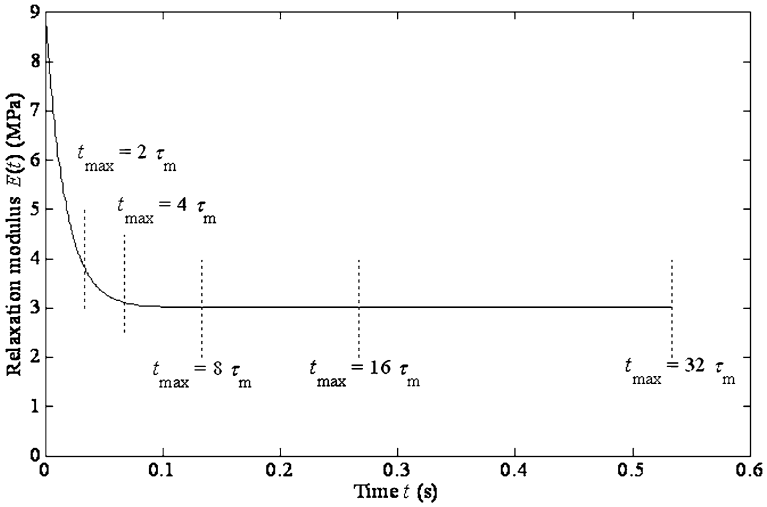

(a)

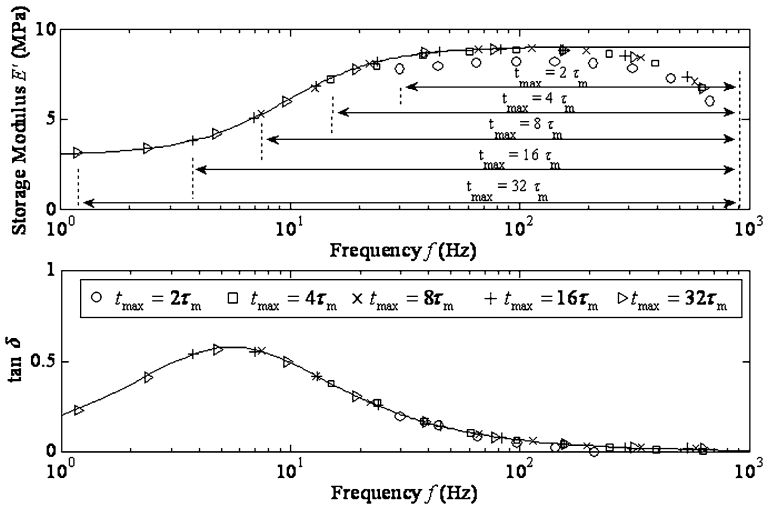

(b)

Fig. 5 Influence of the analyzed time range, conversion from time to frequency. (**a**) Analytic generalized Maxwell model relaxation modulus $E(t)$ provided by Eq. (11), in which different truncation times are illustrated; (**b**) comparison between generalized Maxwell model complex modulus $E^*(\omega)$ provided by Eq. (13) and the result provided by the proposed interconversion method for the different truncation times

and

$$\bar{E}^*(\omega) = E^*(\omega) + \alpha^*(\omega). \tag{20}$$

Then, these generated data have been resampled in order to obtain evenly spaced data $\bar{E}_{\text{es}}(t)$ and $\bar{E}^*_{\text{es}}(\omega)$. For the present case, linear interpolation has been applied.

For the present numerical application, $\Delta t = 10^{-4}$ s and $t_{\max} = 1$ s are used. Figure 7 shows the conversion from relaxation modulus $E(t)$ to complex modulus $E^*(\omega)$. Figure 7(a)

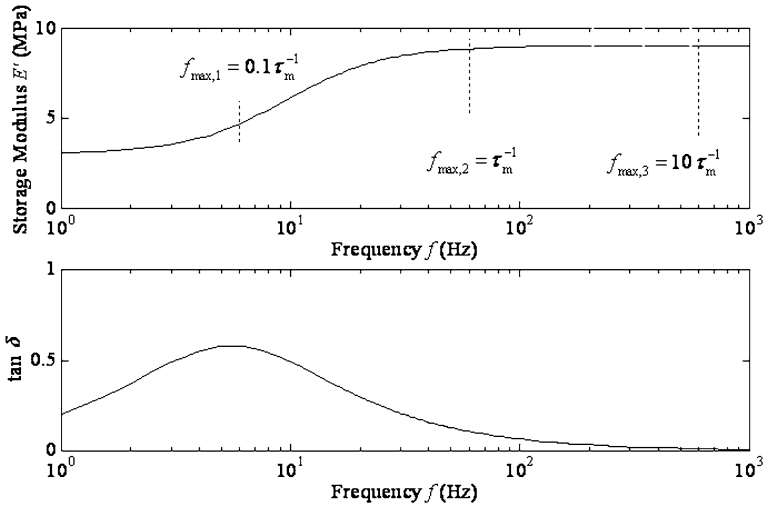

(a)

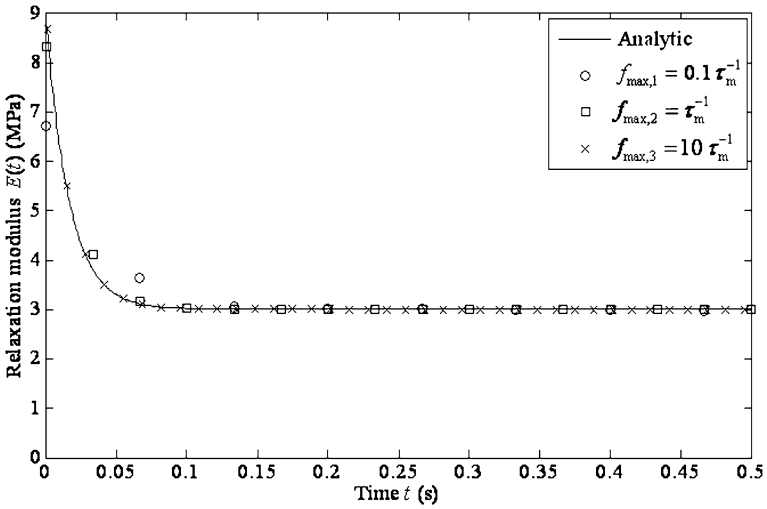

(b)

Fig. 6 Influence of the analyzed frequency range, conversion from frequency to time. (**a**) Analytic generalized Maxwell model complex modulus $E^*(\omega)$ provided by Eq. (13), in which different truncation frequencies are illustrated; (**b**) comparison between generalized Maxwell model relaxation modulus $E(t)$ provided by Eq. (11) and the result provided by the proposed interconversion method for different truncation frequencies

illustrates Eq. (11) together with the pseudo-experimental data $\bar{E}(t)$ and Fig. 7(b) illustrates the converted modulus with the analytic solution for $E^*(\omega)$ given by Eq. (13).

From Fig. 7(b) it should be pointed out that the low-frequency range is properly reproduced while the estimation of $E^*(\omega)$ for the higher frequencies differs from the analytic one given in Eq. (13). This is due to the fact that few points were taken in $E(t)$ during the relaxation, and therefore, a linear interpolation technique is not sufficient to reproduce the employed model. Consequently, a higher number of data points are needed, especially

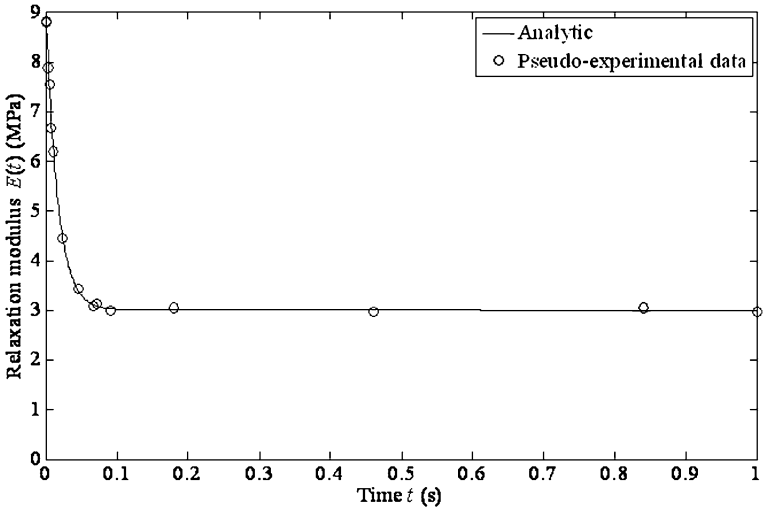

(a)

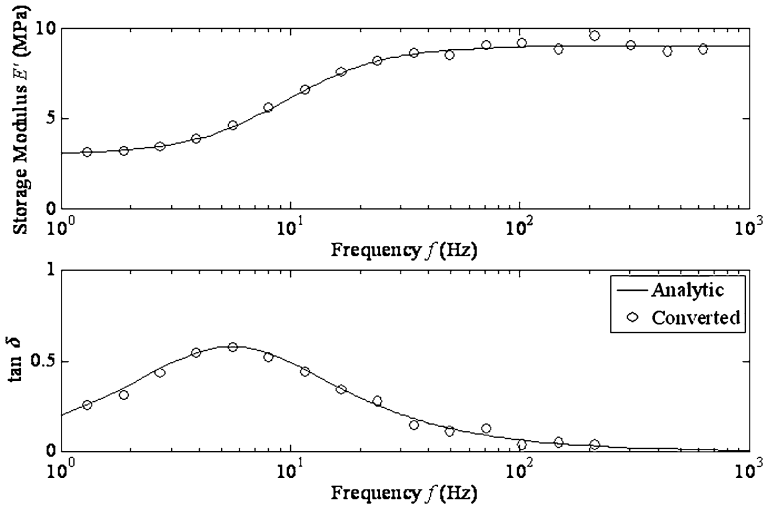

(b)

Fig. 7 Influence of data dispersion, conversion from time to frequency. (**a**) Analytic generalized Maxwell model relaxation modulus $E(t)$ provided by Eq. (11) together with the employed unevenly spaced data; (**b**) comparison between analytic generalized Maxwell model complex modulus $E^*(\omega)$ provided by Eq. (13) and the converted one using data dispersion

during the relaxation. Besides, a higher order interpolation technique will provide better accuracy.

Regarding the inverse conversion, $\Delta f = 0.5$ Hz and $f_{\max} = 1$ kHz are chosen to guarantee a wider time range. Figure 8 shows the conversion from complex modulus to relaxation modulus. Figure 8(a) illustrates Eq. (13) with the pseudo experimental data $\bar{E}^*(\omega)$, and Fig. 8(b) illustrates the converted modulus with the analytical solution for $E(t)$ given by Eq. (11).

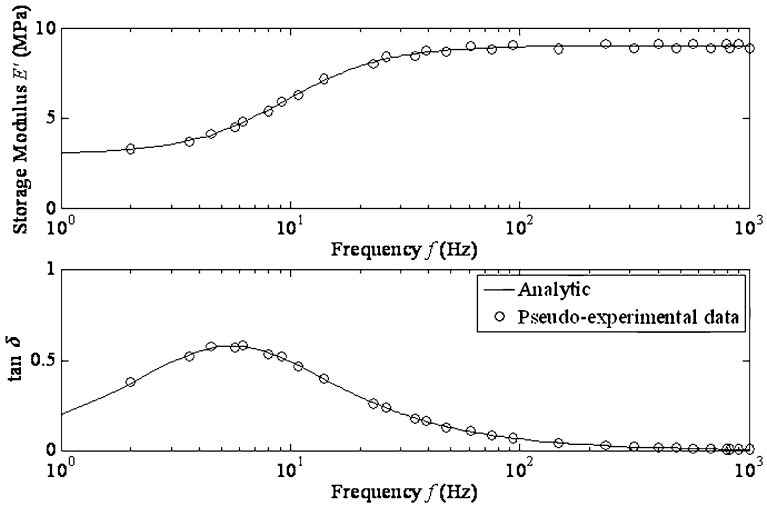

(a)

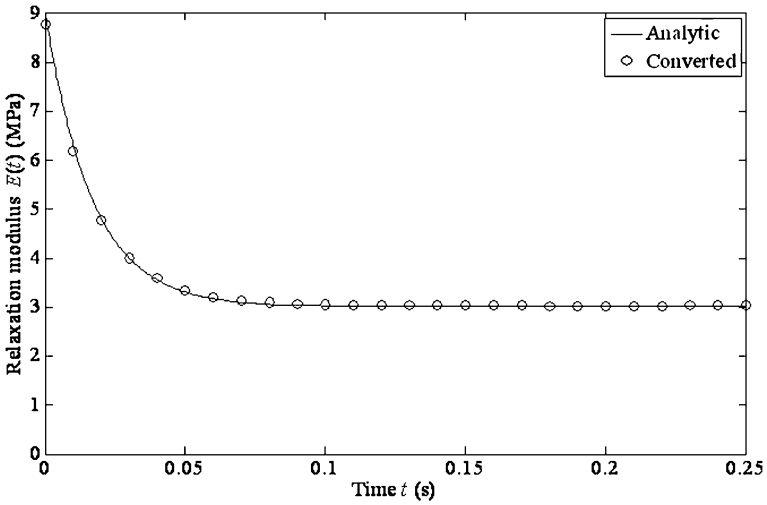

(b)

Fig. 8 Influence of data dispersion, conversion from frequency to time. (**a**) Analytic generalized Maxwell model complex modulus $E^*(\omega)$ provided by Eq. (13) together with the employed unevenly spaced data; (**b**) comparison between analytic generalized Maxwell model relaxation modulus $E(t)$ provided by Eq. (11) and the converted one using data dispersion

From Fig. 8(b) it should be remarked that the converted relaxation modulus precisely matches the response provided by Eq. (11).

In short, it can be concluded that the proposed procedure is capable of providing an accurate estimation of the complex modulus $E^*(\omega)$ and of the relaxation modulus $E(t)$ even though the original data do not match the exact response and even though data are not properly spaced.

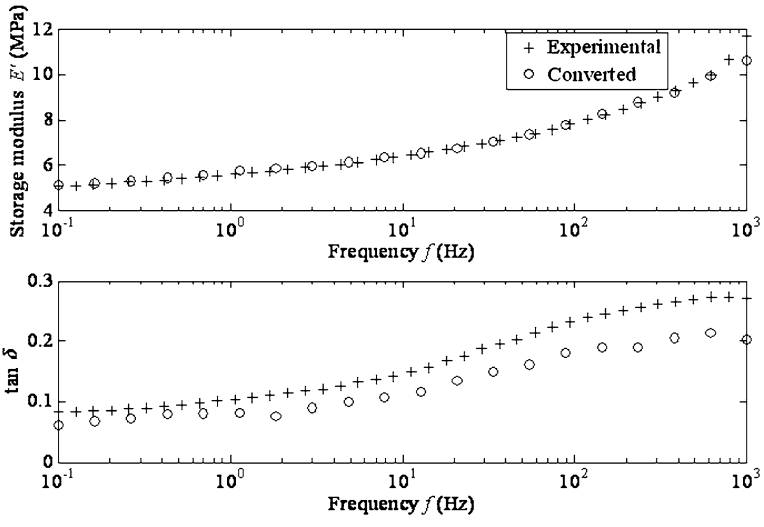

(a)

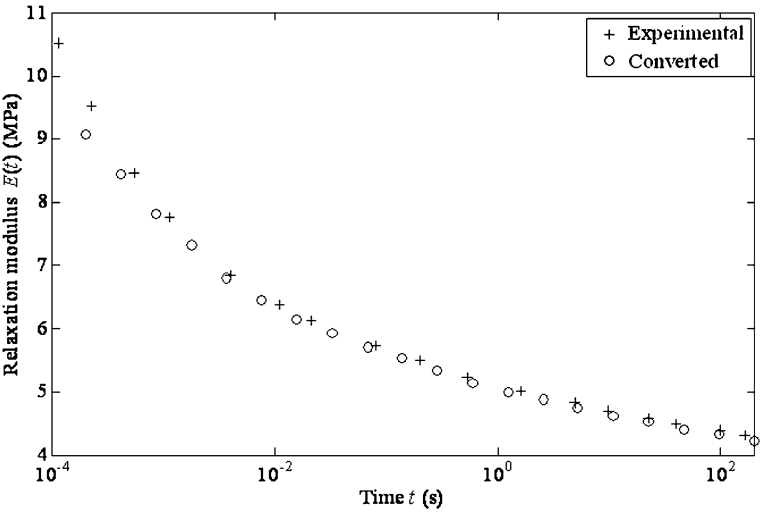

(b)

Fig. 9 Application example using experimental results. (**a**) Conversion from time to frequency: comparison between the experimental complex modulus $E^*(\omega)$ of a flexible adhesive and the converted one from its respective experimental relaxation modulus $E(t)$; (**b**) conversion from frequency to time: comparison between the experimental relaxation modulus $E(t)$ of a flexible adhesive and the converted one from its respective experimental complex modulus $E^*(\omega)$

4 Application example using experimental data

Finally, an application example is presented in which experimental data for DMTA obtained relaxation and complex moduli $E_{\text{exp}}(t)$ and $E^*_{\text{exp}}(\omega)$ of a flexible adhesive (García-Barruetabeña et al. 2011) are used to assess the present procedure. The employed flexible adhesive is a modified sylane. Concretely, ISR 70-03 is employed (Bostik Industry 2010). It

should be remarked that the behavior of the employed material was fitted to an exponential relaxation model (García-Barruetabeña et al. 2011) including nine relaxation functions.

The experimental relaxation modulus $E_{\text{exp}}(t)$ covers the time range 10^{-5} s–3×10^{3} s while the complex modulus $E^*_{\text{exp}}(\omega)$ covers the frequency range 10^{-1} Hz–7×10^{2} Hz. It should be remarked that an interpolation technique is needed to obtain the evenly spaced data. As well, this interpolation step is needed to reach the desired t_{max} and Δt. Concretely, cubic interpolation is used. It should be pointed out that, due to the fact that $E_{\text{exp}}(t)$ and $E^*_{\text{exp}}(\omega)$ are the experimental data, there is no relaxation time τ_{m} associated with them and as a result there is no underlying model. Thus, the desired Δt is estimated using the criteria $\tau_{\text{m}} = 0.66 t_{\text{r}}$ where t_{r} is the elapsed time from the moment the strain is applied until the relaxation is reached. Therefore, $\Delta t = 10^{-5}$ s is derived. Regarding the dynamic case, $\Delta f = 0.01$ Hz is employed. Consequently, Fig. 9(a) compares the conversion from relaxation modulus $E(t)$ to complex modulus $E^*(\omega)$ with the experimental data and Fig. 9(b) shows the inverse conversion.

From Fig. 9(a) it should be noted that the presented methodology provides an accurate prediction for $E^*_{\text{exp}}(\omega)$. On the one hand, concerning the storage modulus, the proposed methodology reproduces the experimental data in the whole frequency range. On the other hand, regarding the loss factor $\tan\delta(\omega)$, the method reproduces the tendency of the experimental data but differences are found, especially in the high-frequency range. These differences are smaller than 5 % for the low-frequency range but up to 30 % for the highest frequencies. However, if a smaller Δt is used, the accuracy of the interconversion will increase. Concerning the interconversion from complex modulus to relaxation modulus, as seen in Fig. 9(b), it should be remarked that the presented procedure provides an accurate prediction for the experimentally obtained relaxation modulus during the relaxation. Nevertheless, an error of 7 % is encountered for the upper time limit. This error can be reduced, as it was discussed on Sect. 3, using a smaller Δf for the interpolation step or starting from a wider frequency range, i.e. employing a higher f_{max} .

5 Concluding remarks

In this paper the interconversion between the relaxation modulus $E(t)$ and the corresponding complex modulus $E^*(\omega)$ for linear viscoelastic materials has been explored. In contrast to other approximate methods, in this work the FFT algorithm proposed by Cooley and Tuckey has been directly applied to time-dependent part of the viscoelastic response $R(t)$. Influences of leakage, signal discretization and analyzed ranges, as well as the eventual experimental error and data dispersion, have been analyzed via an analytical material model. Finally, an application example using experimental data has been carried out to assess the method. As a result, the proposed procedure allows obtaining the complex modulus $E^*(\omega)$ by means of relaxation tests, and vice versa.

Acknowledgements The work presented in this paper has been carried out with the generous financial support from ORONA EIC in Spain.

References

Adhikari, S.: Damping models for structural vibration. Ph.D. Thesis, Cambridge University, Engineering Department (2000)

Adhikari, S.: Classical normal modes in non-viscously damped linear systems. AIAA J. **39**(5), 1–3 (2001)

ASTM E 756-04: Standard test method for measuring vibration damping properties of materials. American Society for Testing and Materials (2004)
Bellanger, M.: Digital Processing of Signals: Theory and Practice. Wiley-Interscience, New York (1984)
Boltzmann, L.: On the theory of the elastic aftereffect. Poggendorff's Ann. Phys. Chem. **7**, 624–645 (1876)
Bostik Industry, Technical Sheet for Industrial Special Range (ISR) 70-03 English version. http://www.bostikindustrie.nl. Consulted on 15th December (2010)
Chen, T.: Determining a Prony series for a viscoelastic material from time varying strain data. NASA Center for AeroSpace Information (CASI) (2000)
Cooley, J., Tukey, J.: An algorithm for the machine calculation of complex Fourier series. Math. Comput. **19**, 297–301 (1965)
Dutt, A., Rokhlin, V.: Fast Fourier transforms for nonequispaced data II. Appl. Comput. Harmon. Anal. **2**, 85–100 (1995)
Emri, I., von Bernstorff, B.S.: Re-examination of the approximate methods for interconversion between frequency- and time-dependent material functions. J. Non-Newton. Fluid Mech. **129**, 75–84 (2005)
Fernández, P., Rodriguez, D., Lamela, M., Fernández-Canteli, A.: Study of the interconversion between viscoelastic behaviour functions of PMMA. Mech. Time-Depend. Mater. **15**(2), 169–180 (2011)
Ferry, J.D.: Viscoelastic Properties of Polymers, 3rd edn. Wiley, New York (1980)
Fourmont, K.: Non-equispaced fast Fourier transforms with applications to tomography. J. Fourier Anal. Appl. **9**, 431–450 (2003)
García-Barruetabeña, J., Cortés, F., Abete, J.M., Fernández, P., Lamela, M.J., Fernández-Cantelli, A.: Mechanical behavior experimental characterization and modelization of a flexible adhesive. Mater. Des. **32**, 2783–2796 (2011)
Greengard, L., Lee, J.Y.: Accelerating the nonuniform fast Fourier transform. SIAM Rev. **46**(3), 443–454 (2004)
Jahani, K., Nobari, A.: Identification of dynamic (Young's and shear) moduli of a structural adhesive using modal based direct model updating method. Exp. Mech. **48**, 599–611 (2008)
Kulik, V.M., Semenov, B.N., Boiko, A.V., Seoudi, B.M., Chun, H.H., Lee, I.: Measurement of dynamic properties of viscoelastic materials. Exp. Mech. **49**, 417–425 (2009)
Leblanc, J.: Fourier transform rheometry: A new tool to investigate intrinsically non-linear viscoelastic materials. Annu. Trans. Nord. Rheol. Soc. **13**, 3–21 (2005)
Lee, J.Y., Greengard, L.: The type 3 nonuniform FFT and its applications. J. Comput. Phys. **206**, 1–5 (2005)
Maheri, M.R., Adams, R.D.: Determination of dynamic shear modulus of structural adhesives in thick adherent shear test specimens. Int. J. Adhes. Adhes. **22**, 119–127 (2002)
Marion, D.: Fast acquisition of NMR spectra using Fourier transform of non-equispaced data. J. Biomol. NMR **32**, 141–150 (2005)
Nashif, A.D., Jones, D.I.G., Henderson, J.P.: Vibration Damping. Wiley Interscience, New York (1985)
Ninomiya, K., Ferry, J.D.: Some approximate equations useful in the phenomenological treatment of linear viscoelastic data. J. Colloid Interface Sci. **14**, 36–48 (1959)
Oran, B.: The Fast Fourier Transform and Its Applications. Pretince Hall International, Englewood Cliffs (1988)
Park, S.W., Schapery, R.A.: Methods of interconversion between linear viscoelastic material functions. Part I–A numerical method based on Prony series. Int. J. Solids Struct. **36**, 1653–1675 (1999a)
Park, S.W., Schapery, R.A.: Methods of interconversion between linear viscoelastic material functions. Part II–An approximate analytical method. Int. J. Solids Struct. **36**, 1677–1699 (1999b)
Schwarzl, F.: On the interconversion between viscoelastic material functions. Pure Appl. Chem. **23**, 219–234 (1970)
Sjöberg, M., Kari, L.: Nonlinear isolator dynamics at finite deformations: an effective hyperelastic, fractional derivative, generalized friction model. Nonlinear Dyn. **33**, 323–336 (2003)
Sorvari, J., Malinen, M.: Numerical interconversion between linear viscoelastic material functions with regularization. Int. J. Solids Struct. **44**, 1291–1303 (2007)
Ward, I.M., Sweeney, J.: An Introduction to the Mechanical Properties of Polymers. Wiley, New York (2004)
Warnaka, G.E., Miller, H.T.: Strain-frequency-temperature relationships in polymers. J. Eng. Ind., B **90**(3), 491–498 (1968)